

Article

Enhancing the Reduction of High-Aluminum Iron Ore by Synergistic Reducing with High-Manganese Iron Ore

Xianlin Zhou ^{1,2,3} , Yanhong Luo ^{1,3,*}, Tiejun Chen ^{1,3} and Deqing Zhu ^{2,*}

¹ Hubei Key Laboratory for Efficient Utilization and Agglomeration of Metallurgic Mineral Resources, Wuhan University of Science and Technology, Wuhan 430081, China; xlzhou@wust.edu.cn (X.Z.); chentiejun@wust.edu.cn (T.C.)

² School of Mineral Processing and Bioengineering, Central South University, Changsha 410083, China

³ School of Resource and Environmental Engineering, Wuhan University of Science and Technology, Wuhan 430081, China

* Correspondence: yhluo@wust.edu.cn (Y.L.); dqzhu@csu.edu.cn (D.Z.);
Tel.: +86-027-6886-2204 (Y.L.); +86-731-8883-6942 (D.Z.)

Received: 29 November 2018; Accepted: 19 December 2018; Published: 22 December 2018



Abstract: How to utilize low grade complex iron resources is an issue that has attracted much attention due to the continuous and huge consumption of iron ores in China. High-aluminum iron ore is a refractory resource and is difficult to upgrade by separating iron and alumina. An innovative technology involving synergistic reducing and synergistic smelting a high-aluminum iron ore containing 41.92% Fe_{total}, 13.74% Al₂O₃, and 13.96% SiO₂ with a high-manganese iron ore assaying 9.24% Mn_{total} is proposed. The synergistic reduction process is presented and its enhancing mechanism is discussed. The results show that the generation of hercynite (FeAl₂O₄) and fayalite (Fe₂SiO₄) leads to a low metallization degree of 66.49% of the high-aluminum iron ore. Over 90% of the metallization degree is obtained by synergistic reducing with 60% of the high-manganese iron ore. The mechanism of synergistic reduction can be described as follows: MnO from the high-manganese ore chemically combines with Fe₂SiO₄ and FeAl₂O₄ to generate Mn₂SiO₄, MnAl₂O₄ and FeO, resulting in higher activity of FeO, which can be reduced to Fe in a CO atmosphere. The main products of the synergistic reduction process consist of Fe, Mn₂SiO₄, and MnAl₂O₄.

Keywords: high-aluminum iron ore; synergistic reduction; high-manganese iron ore; hercynite; fayalite

1. Introduction

In 2017, 87.47% of 1229 million tons of iron ore consumed by the Chinese iron steel industry were imported [1]. With the increasing consumption of good-quality iron ores, the poor, fine, and complex domestic iron ore resources cannot meet the huge demand of the iron and steel industry in China. Thus, it is important to utilize low grade iron resources efficiently [2], such as high-aluminum iron resources including high-aluminum limonite and red mud, which is a residue generated after the clarification of bauxite [3].

High-aluminum iron ore is a typical refractory iron resource, which is difficult to upgrade by physical processes due to the superfine size and close dissemination of iron minerals with gangue minerals [4]. Some were directly used as a sintering raw material at a low ratio, which affected the sintering process adversely [5]. Therefore, many separating approaches have been published for high-aluminum iron resources, which can be classified as: (1) physical processes like gravity concentration and magnetic separation [6,7] and flotation [8], (2) pyrometallurgical processes containing solid-state reduction [4,9–12], and smelting [12–15]. So far, iron and aluminum cannot be

separated completely by physical processes and flotation processes, and more than 10% of sodium additive is required by the solid-state sodium roasting process, leading to a high risk of the degradation of refractory materials in furnaces [16] and higher costs. In the smelting process, iron ore was mixed with coal and binder to make briquettes and then smelted in a melter to separate the iron and slag over 1550 °C [17], where iron and aluminum can be isolated entirely. Nevertheless, Al_2O_3 affects the viscosity and desulfurizing capacity of blast furnace slag a lot [18], causing a limit usage of the high-aluminum resources in a blast furnace. In order to elevate the ratio of high-aluminum iron resources in the smelting process, a novel technology of synergistic reducing and synergistic smelting the high-aluminum iron ore with a high-manganese iron ore is proposed, and the synergistic reduction process is presented in this paper to discuss its enhancing mechanism.

2. Materials and Methods

2.1. Raw Materials

The chemical analysis of a high-aluminum iron ore (HA ore) and a high-manganese iron ore (HM ore) are given in Table 1. The two iron ores are both low iron grade, and the HA ore contains high contents of alumina and silica, while high manganese content was observed in the HM ore, assaying 9.24%. XRD results in Figure 1 illustrate that iron minerals in the two ores consist of hematite and goethite, the aluminum and silica minerals are kaolinite and gibbsite, and the manganese mineral in the HM ore is pyrolusite. Former results showed that hematite in the HA ore is closely included with kaolinite [19]. Figure 2 indicates that iron mineral is surrounded by kaolinite, and that pyrolusite and kaolinite are closely associated with each other. Complex mineral compositions and microstructures in the two iron ores led to significant difficulties in the separation of iron and gangue.

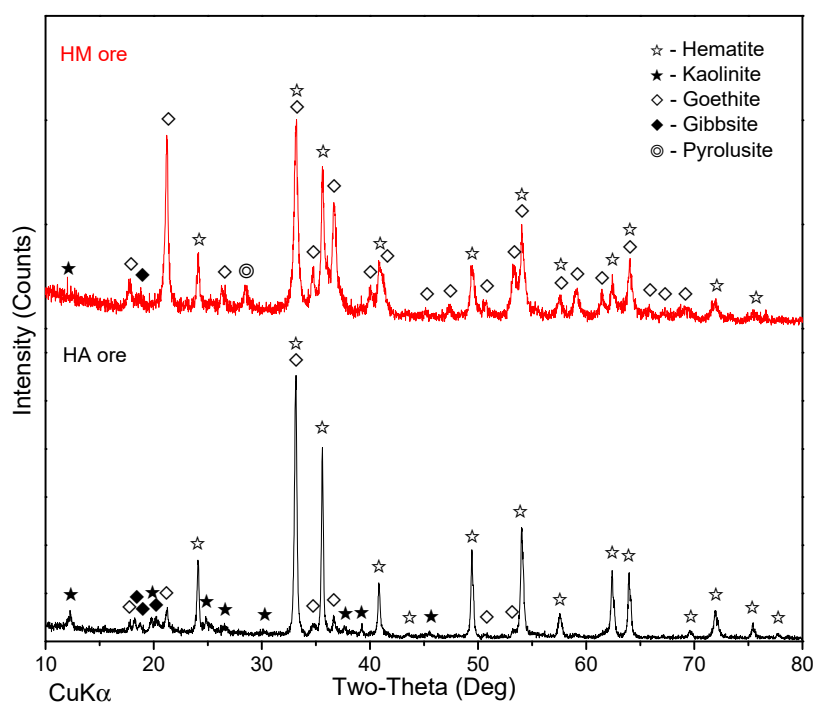


Figure 1. X-ray diffraction (XRD) pattern of high-aluminum iron ore (HA ore) and high-manganese iron ore (HM ore).

A soft coal was used as the reducer during the tests, which contained 52.12% fixed carbon on an air dry basis (FC_{ad}), 30.41% volatile matter on a dry ash free (V_{daf}) basis, 4.49% ash on an air dry basis (A_{ad}), 0.58% S and a melting temperature of 1376 °C. The size distribution of the soft coal is 100%, passing at 5 mm.

Table 1. Chemical compositions of raw materials (wt. %).

Ores	Fe _{total}	Mn _{total}	Al ₂ O ₃	SiO ₂	CaO	MgO	Pb	Zn	P	S	LOI
High-aluminum iron ore (HA ore)	41.92	1.24	13.74	13.96	0.13	0.88	0.64	0.21	0.130	0.014	7.20
High-manganese iron ore (HM ore)	42.32	9.24	6.60	4.22	0.20	0.20	1.86	0.98	0.065	0.018	11.05

Note: LOI, loss on ignition.

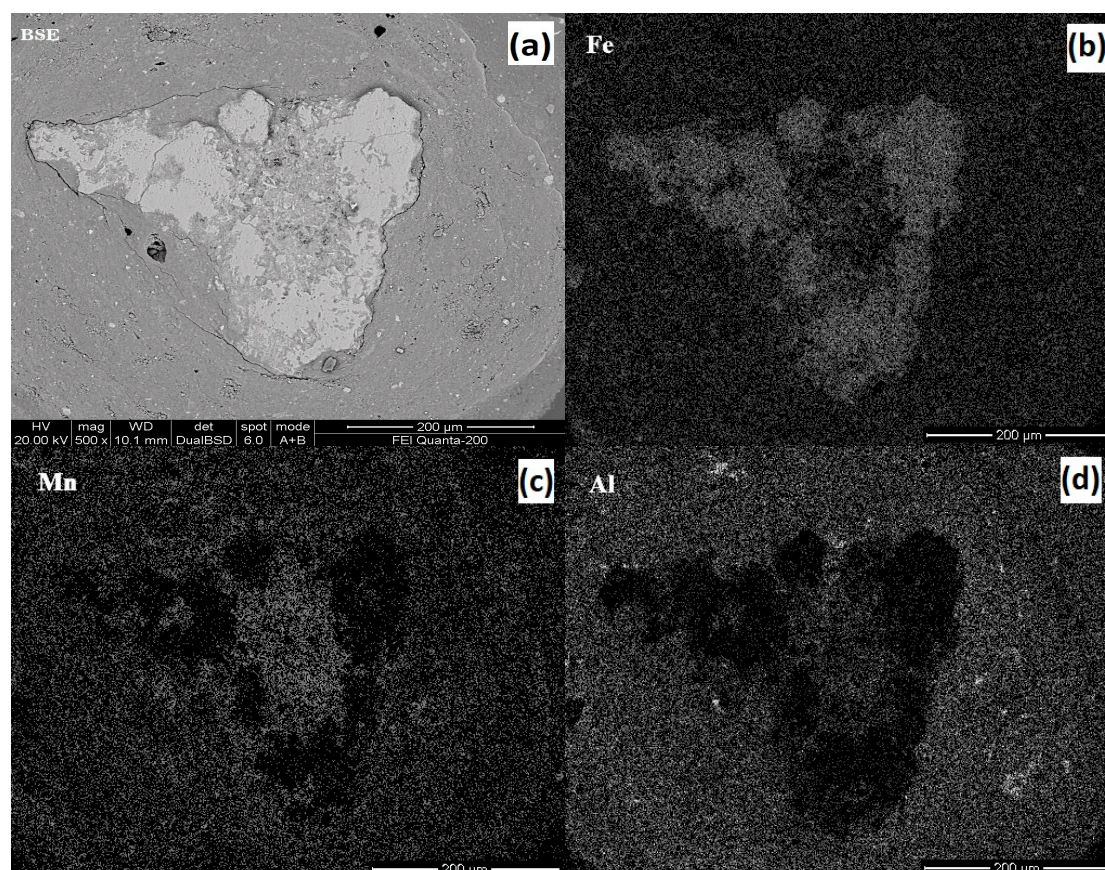


Figure 2. Representative SEM-BSE micrographs of HM ore. (BSE in (a), Back Scattered Electron Imaging; Fe element in (b); Mn element in (c); Al element in (d)).

2.2. Experimental Procedures

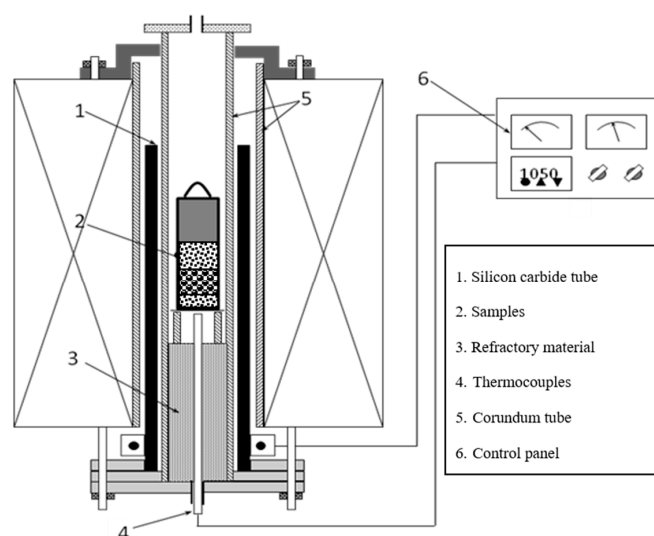
The reduction process includes procedures as follows: mixing the two iron ores at a given ratio, pelletizing of the mixture, and reduction roasting of dried pellets. Different experimental conditions of the reduction tests are summarized in Table 2.

Mixtures were prepared by mixing the two iron ores under different ratios, where the fraction of added HM ore is referred to the mixture of two ores. Then, green balls were made by balling the mixtures in a disc pelletizer of 0.8 m in diameter and a 0.2 m rim depth, rotating at 38 rpm and being inclined at 47° to the horizontal. The screened green balls of 8–16 mm were loaded into the drying oven to dry at 105 °C for 2 h until the weight was unchanged.

The dried pellets were put into a stainless steel crucible and covered by some soft coal, where the mass of soft coal was determined by the C/Fe mass ratio, which was calculated on the whole available iron content of the pellets. The crucible was loaded into a vertical furnace diagrammed in Figure 3 (model: SK-8-13, The Great Wall Furnace, Changsha, China) and roasted for a given reduction time while the reducing temperature was elevated to the target value. After that, the reduced pellets were unloaded and cooled down by covering with pulverized coal.

Table 2. Different experimental conditions of the reduction tests.

Series No.	High-Aluminum Iron Ore: High-Manganese Iron Ore (HA:HM) Ratio	C/Fe Mass Ratio	Temperature	Reduction Duration
1	100:0	1.5	800 °C, 850 °C, 900 °C, 950 °C, 1000 °C, 1050 °C, 1100 °C	60 min
2	100:0	1.5	1050 °C	15 min, 30 min, 45 min, 60 min, 75 min, 90 min, 120 min
3	100:0	0.5, 1.0, 1.5, 2.0	1050 °C	90 min
4	100:0, 80:20, 60:40, 40:60, 20:80, 0:100	1.5	1050 °C	90 min

**Figure 3.** Schematic of vertical furnace for reduction.

X-ray fluorescence spectroscopy (XRF, PANalytical Axios mAX, PANalytical B.V., Almelo, The Netherlands) and chemical analysis were applied for the chemical compositions of raw materials and the reduced pellets. The crystalline phase compositions of the materials were detected by an X-ray diffractometer (XRD, D/Max-2500, Rigaku Co., Tokyo, Japan). Proximate analysis of coal was conducted by the Chinese standards GB/T212-2008. Microstructures of raw materials were observed by a scanning electron microscope (SEM, FEI Quanta-200, FEI Company, GG Eindhoven, The Netherlands) and an optical microscope (DMI4500P, Leica, Wetzlar, Germany), respectively. The compositional analyses were carried out using an energy dispersion system (EDAX-TSL, Ametek Inc., Paoli, CO, USA) within the SEM. Microstructures of reduced pellets were observed by an optical microscope. Metallization degree was applied to evaluate the reduction results, where the metallization degree was determined by the ratio between metallic iron on total iron of the reduced pellets according to ISO 11258:2015.

3. Results

3.1. Effect of Reduction Temperature

The single HA ore pellets were reduced by optimizing the reduction parameters, to reveal the reducibility of HA ore. The effect of reduction temperature on the metallization degree of HA reduced pellets is shown in Figure 4 under reducing for 60 min with C/Fe mass ratio of 1.5. It was discovered that the metallization degree rose at first, then decreased, and the peak appeared at 1050 °C. Only 53.68% of the best value of the metallization degree was obtained, declaring a weak reducibility of the HA ore.

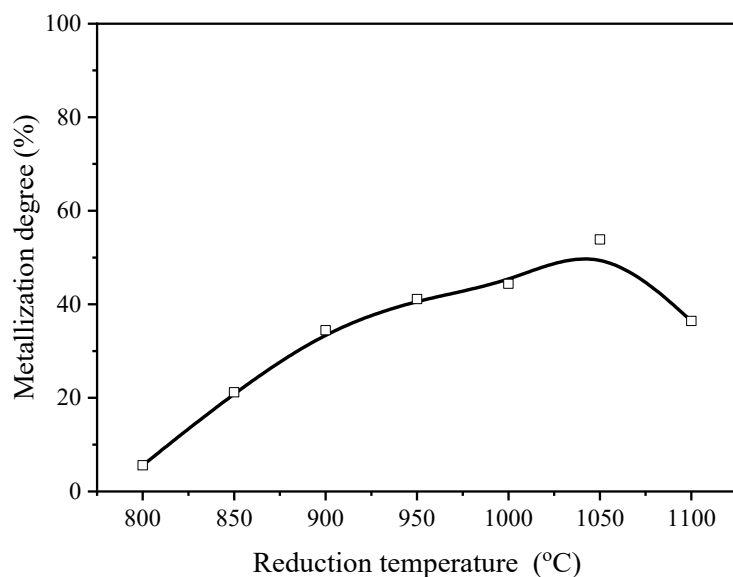


Figure 4. Effect of reduction temperature on metallization degree of reduced pellets of high-aluminum iron ore (HA ore) (reducing for 60 min with C/Fe mass ratio of 1.5).

3.2. Effect of Reduction Duration

Figure 5 presents the reduction duration effect result on the metallization of reduced pellets. By prolong the reduction from 15 min to 30 min, an obvious improvement from 41.86% to 55.29% is achieved. Generally, a subtle enhanced trend is found. However, still low metallization degrees are shown in Figure 5. Only 66.49% of the metallization degree is obtained by reducing the HA pellets for 120 min, which is far lower than that of high grade iron concentrate pellets [20].

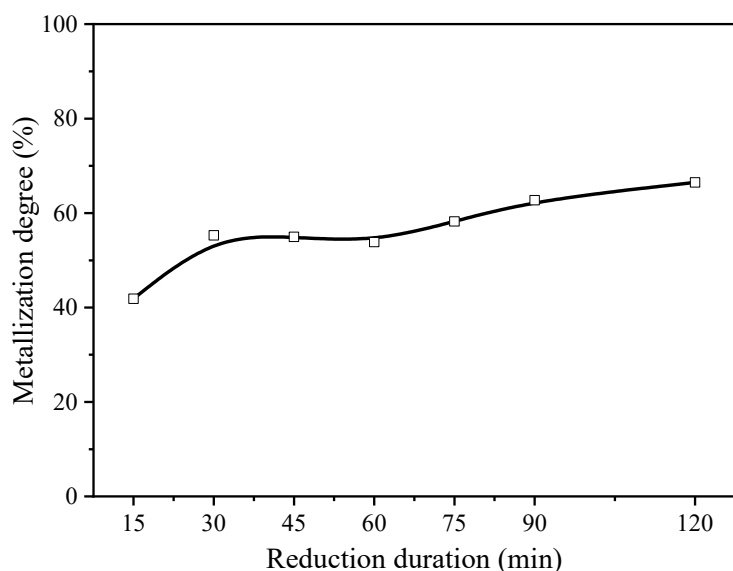


Figure 5. Effect of reduction duration on metallization of reduced pellets of high-aluminum iron ore (HA ore) (reducing at 1050 °C with C/Fe mass ratio of 1.5).

3.3. Effect of Reductant Ratio

As shown in Figure 6, the metallization degree of reduced pellets of HA ore increases slightly and then remains steady when the C/Fe mass ratio is elevated from 0.5 to 2.0. However, only part of the iron was reduced to metallic iron, where the best value only 62.72% is obtained.

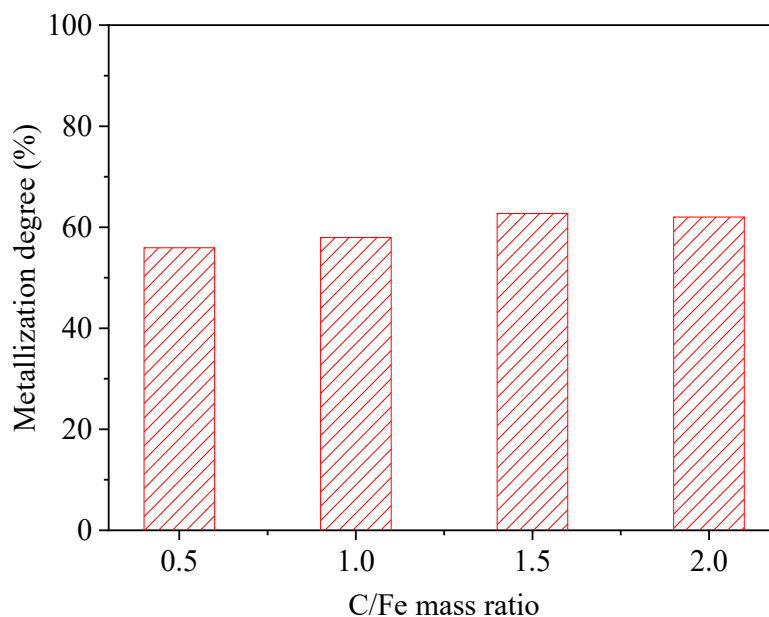


Figure 6. Effect of C/Fe mass ratio on metallization of reduced pellets of high-aluminum iron ore (HA ore) (reducing at 1050 °C for 90 min).

3.4. Effect of HM Ore Ratio

From the above optimization results of the reduction process, it can be concluded that the HA ore has poor reducibility. Thus, the HM ore was blended with the HA ore to investigate the effect of HM ore on the reduction behavior of HA ore. It can be observed from Figure 7 that the metallization degree increases continuously by raising the HM ore ratio. Meanwhile, the reduction of pellets is promoted by prolonging the reduction duration. The distributions of metallic iron grains in Figure 8 signify that more obvious iron grains form by blending with more HM ore.

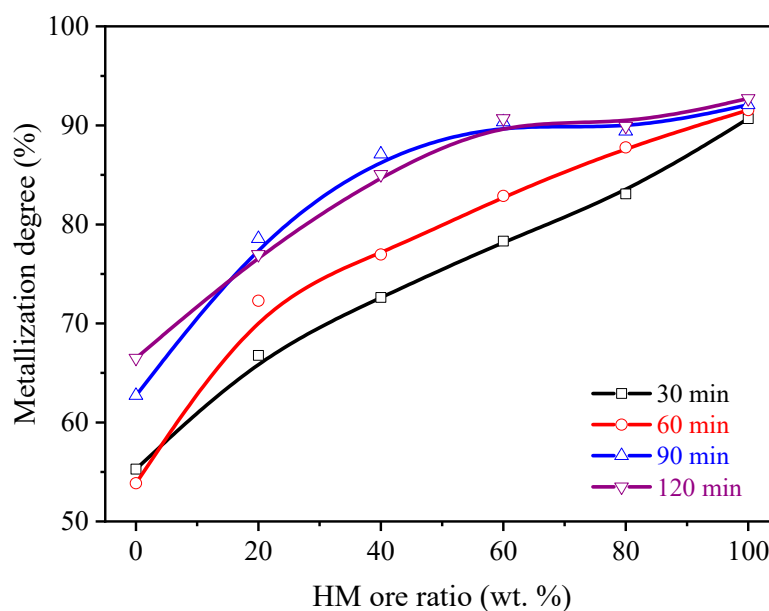


Figure 7. Effect of ratio of high-manganese iron ore (HM ore) in blend on metallization degree of reduced pellets (reducing at 1050 °C with C/Fe mass ratio of 1.5).

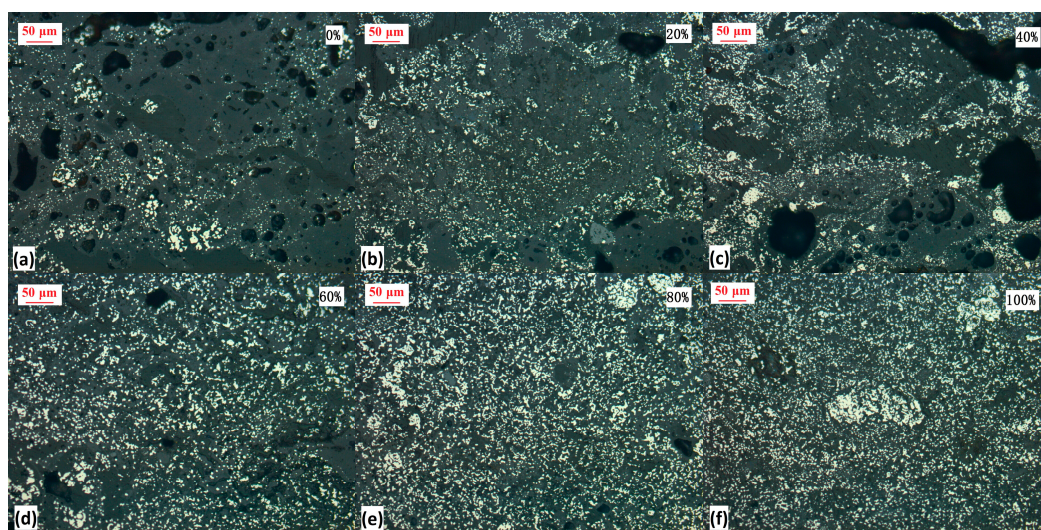


Figure 8. Effect of high-manganese iron ore (HM ore) ratio from 0% to 100% (a–f) on distribution of metallic iron grains (white color) in reduced pellets (reducing at 1050 °C for 90 min with C/Fe mass ratio of 1.5).

4. Discussion

XRD results of HA reduced pellets under different temperatures are illustrated in Figure 9. Note that fayalite can easily form during the reduction of HA ore. Meanwhile, the diffraction peak intensities of hercynite increase sharply with ascending temperatures, while those of fayalite weaken. According to the thermodynamic criterion, both fayalite and hercynite could not be reduced by CO when the temperature ranged from 800 °C to 1100 °C, causing low metallization of HA reduced pellets. Moreover, weaker peak intensity of iron and stronger of fayalite were detected at 1100 °C. Dynamically, the reduction from FeO to Fe is the restrictive step of reduction of iron ore [21]. Thus, there is more probability of forming fayalite by the chemical combination of FeO and SiO₂ during the reduction process, leading to a decrease of the metallization degree of the reduced HA pellets at 1100 °C.

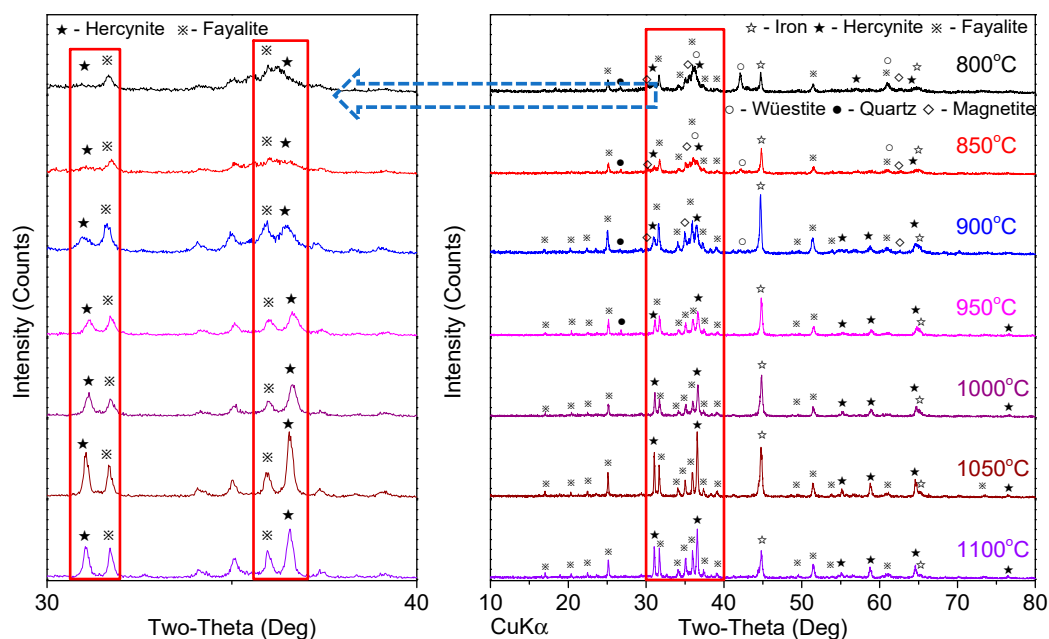


Figure 9. Effect of reduction temperature on mineral compositions of high-aluminum iron ore (HA) reduced pellets (reducing for 60 min with C/Fe mass ratio of 1.5).

A thermodynamic simulation of a system based on the compositions of the HA ore was processed by FactSage7.1 (Thermfact/CRCT, Montreal, QC, Canada; GTT-Technologies, Herzogenrath, Germany), and the result is depicted in Figure 10 as phase fraction as a function of temperature. The simulation is based on reaching equilibrium at every temperature, and only solid phases and gaseous (not shown) are considered. The Fe_2O_3 is already reduced to Fe at 800 °C when the simulation starts. However, Fe_2SiO_4 and FeAl_2O_4 also appear. $\text{Fe}_2\text{Al}_4\text{Si}_5\text{O}_{18}$ appears at 850 °C and the content increases. The largest variation in concentration is at 975 °C, when $\text{Mn}_2\text{Al}_4\text{Si}_5\text{O}_{18}$ totally disappear to the benefit of $\text{Fe}_2\text{Al}_4\text{Si}_5\text{O}_{18}$ and $\text{Mn}_3\text{Al}_2\text{Si}_3\text{O}_{12}$. According to the simulation result, less than 50% of Fe_2O_3 was reduced to Fe by CO between 800 °C to 1100 °C, while other iron was composed of Fe_2SiO_4 , FeAl_2O_4 and $\text{Fe}_2\text{Al}_4\text{Si}_5\text{O}_{18}$. This indicates that it is difficult to further achieve a better metallization degree only by an optimization of a combination of time, temperature, and C/Fe ratio.

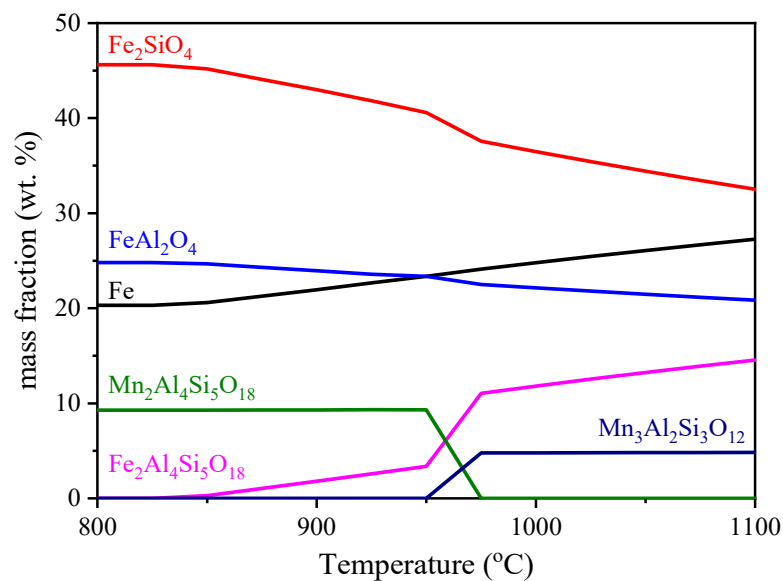


Figure 10. Thermodynamic simulation of a system consisting of Fe_2O_3 , CO, SiO_2 , Al_2O_3 and MnO carried out between 800 °C and 1100 °C in CO atmosphere at ambient pressure.

Combining the experimental results and simulation results, the mechanism of reducing HA ore shown in Figure 11 can be described as follows: (a), the main iron oxide hematite is deoxidized by CO and the intermediate product FeO forms; (b), FeO is reduced to Fe in CO atmosphere; (c), the reduction rate of (b) is slow dynamically [21], and the intermediate product FeO reacts with the gangue minerals SiO_2 and Al_2O_3 to produce Fe_2SiO_4 and FeAl_2O_4 . The main products consist of Fe, Fe_2SiO_4 and FeAl_2O_4 .

As shown in Figure 12, by synergistic reducing with HM ore, hercynite and fayalite are replaced by galaxite and tephroite, respectively. No fayalite but fayalite mangananoan ($(\text{Fe}, \text{Mn})_2\text{SiO}_4$) is detected when the HM ore ratio reaches 40%. Meanwhile, the intensity of hercynite peak gets lower. Thermodynamically, galaxite and tephroite can be generated more easily than hercynite and fayalite, as represented in Figure 13. Thus, FeO can be dissociated from hercynite and fayalite by adding with MnO, where the activity of FeO is improved and the reducibility of HA ore is enhanced.

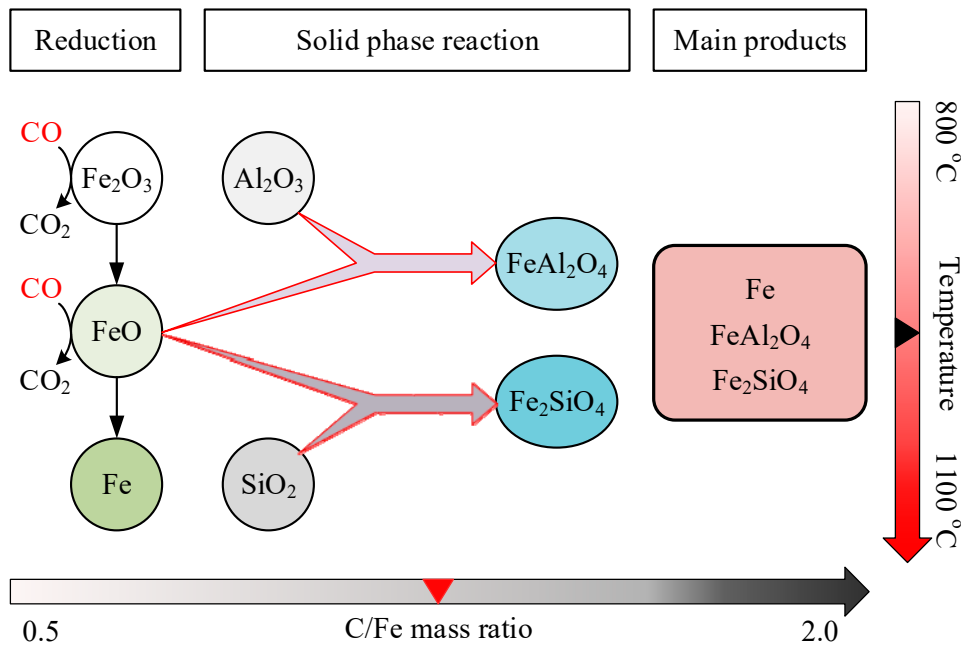


Figure 11. The mechanism of reducing high-aluminum iron ore (HA ore) by CO.

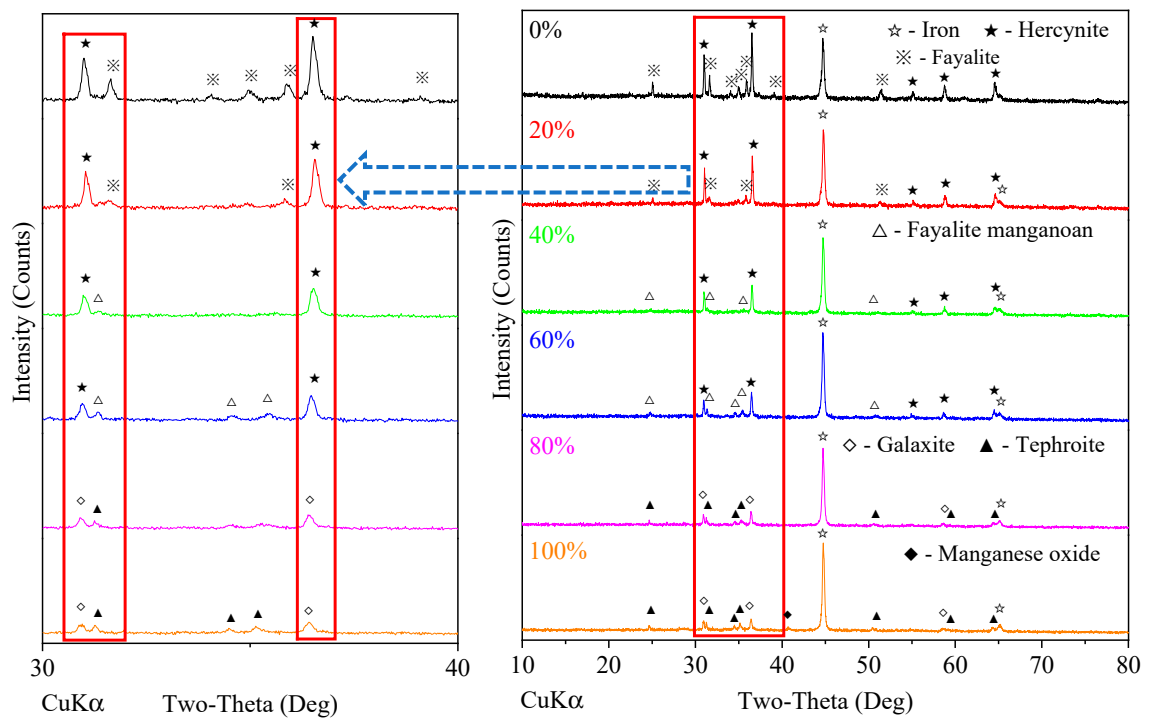


Figure 12. XRD patterns of reduced pellets with different ratio of high-manganese iron ore (HM ore) (reducing at 1050 °C for 90 min with C/Fe mass ratio of 1.5).

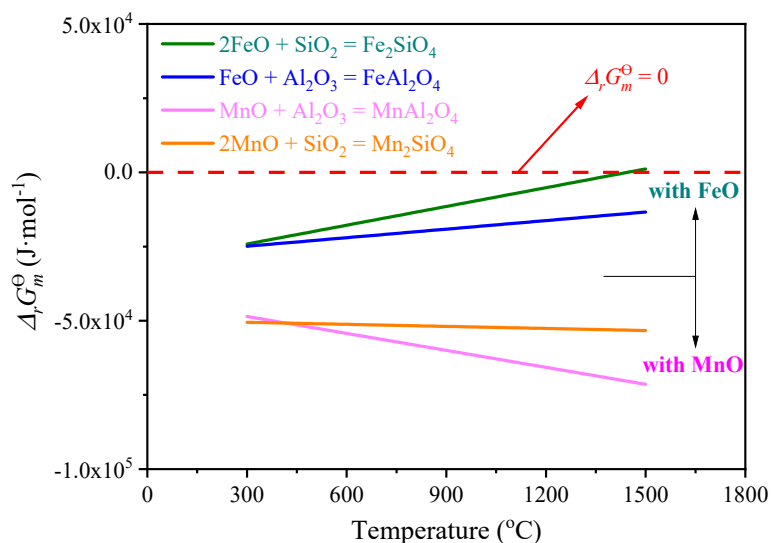


Figure 13. Comparison of standard Gibbs free energy change of reactions between Al_2O_3 and SiO_2 with MnO and FeO.

Another simulation based on the compositions of different HM ore ratio was processed by FactSage7.1, and the results are plotted in Figure 14. Less Fe_2SiO_4 and FeAl_2O_4 are produced by increasing the HM ore ratio, while by contrast, more Fe and Mn-Al-Si compounds are generated.

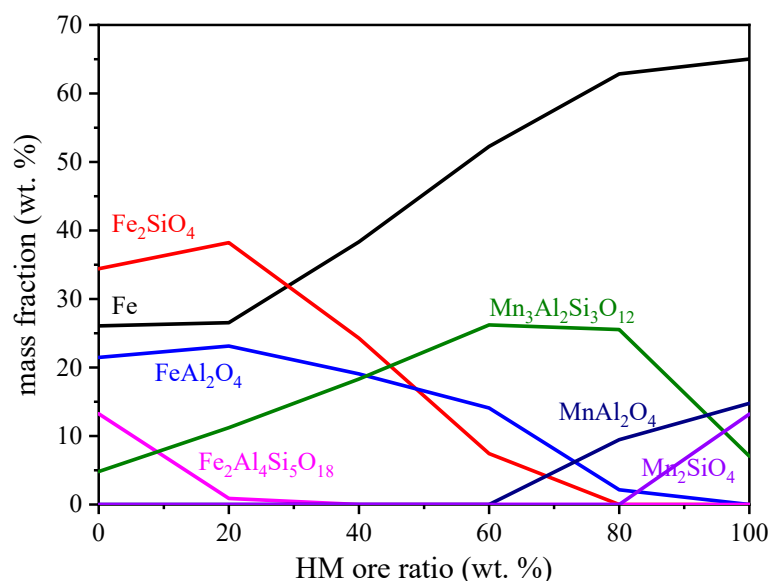


Figure 14. Thermodynamic simulation of a system consisting of Fe_2O_3 , CO, SiO_2 , Al_2O_3 and MnO (with different high-manganese iron ore (HM ore) ratio) carried out at 1050 °C in CO atmosphere at ambient pressure.

Accordingly, the mechanism of synergistic reducing of HA ore and HM ore shown in Figure 15 can be described as follows: (a) The main iron oxide hematite is deoxidized by CO and the intermediate product FeO forms; (b) FeO reacts with the gangue minerals SiO_2 and Al_2O_3 to produce Fe_2SiO_4 and FeAl_2O_4 ; (c) MnO from HM ore combines with Fe_2SiO_4 and FeAl_2O_4 to form Mn_2SiO_4 , MnAl_2O_4 and FeO; (d) FeO is reduced to Fe in CO atmosphere. The main products consist of Fe, Mn_2SiO_4 and MnAl_2O_4 .

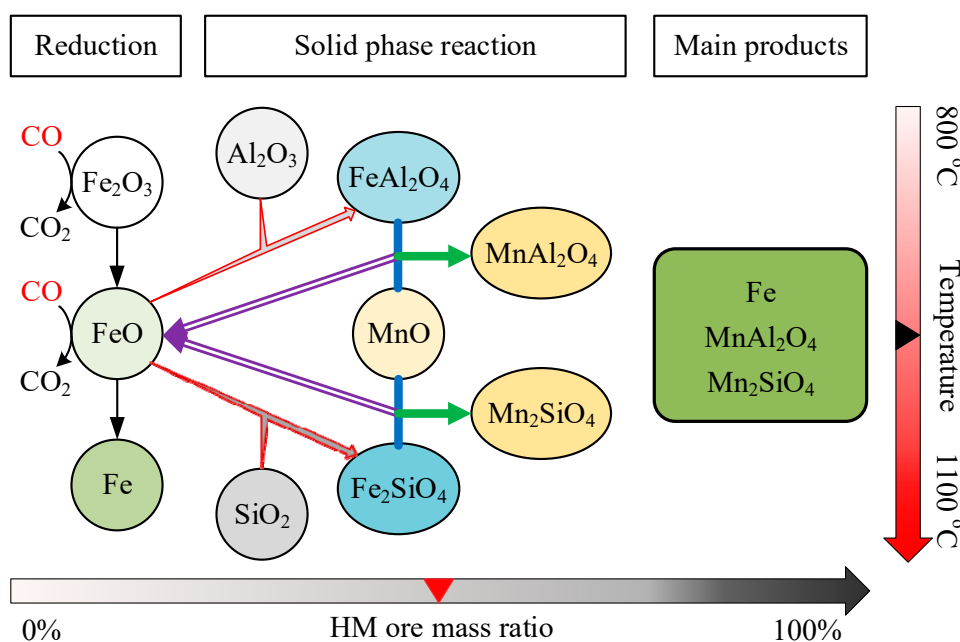


Figure 15. The mechanism of synergistic reducing of high-aluminum iron ore (HA ore) and high-manganese iron ore (HM ore) by CO.

5. Conclusions

In this study, a mechanism for enhancing the reduction of high-aluminum iron ore by synergistic reducing with high-manganese iron ore was investigated. The conclusions can be summarized as follows:

(1) Because of the generation of hercynite and fayalite, only 66.49% of metallization degree is obtained by reducing the high-aluminum iron ore containing 41.92% Fe_{total} , and 13.74% Al_2O_3 under 1050 °C for 120 min with C/Fe mass ratio of 1.5. By synergistic reducing with a high-manganese iron ore assaying 9.24% Mn_{total} , a higher metallization degree is achieved. Over 90% of the metallization degree is obtained by adding with 60% of the high-manganese iron ore.

(2) The mechanism of reducing HA ore can be described as follows: (a) the main iron oxide hematite is deoxidized by CO and the intermediate product FeO forms; (b) FeO reacts with the gangue minerals SiO_2 and Al_2O_3 to produce Fe_2SiO_4 and $FeAl_2O_4$; (c) FeO is reduced to Fe in CO atmosphere. The main products consist of Fe, Fe_2SiO_4 and $FeAl_2O_4$.

(3) The mechanism of synergistic reducing of HA ore and HM ore can be described as: (a) the main iron oxide hematite is deoxidized by CO and the intermediate product FeO forms; (b) FeO reacts with the gangue minerals SiO_2 and Al_2O_3 to produce Fe_2SiO_4 and $FeAl_2O_4$; (c) MnO from HM ore combines with Fe_2SiO_4 and $FeAl_2O_4$ to form Mn_2SiO_4 , $MnAl_2O_4$ and FeO; (d) FeO is reduced to Fe in CO atmosphere. The main products consist of Fe, Mn_2SiO_4 and $MnAl_2O_4$.

Author Contributions: X.Z. and D.Z. conceived of and designed the experiments. X.Z. and Y.L. performed the experiments and analyzed the data. D.Z. contributed materials. X.Z. and Y.L. wrote the paper. D.Z. and T.C. modified the paper.

Funding: This research was funded by Hubei Key Laboratory for Efficient Utilization and Agglomeration of Metallurgic Mineral Resources (No. 2017zy002, No. 2017zy012), Wuhan University of Science and Technology (No. 2017xz013) and National Natural Science Foundation of China (No. 51574281).

Acknowledgments: This work was financially supported by Hubei Key Laboratory for Efficient Utilization and Agglomeration of Metallurgic Mineral Resources, Wuhan University of Science and Technology and National Natural Science Foundation of China.

Conflicts of Interest: The authors declare no conflict of interest.

References

1. World Steel Association Economics Committee. *Steel Statistical Yearbook 2018*; World Steel Association: Brussels, Belgium, 2018; p. 104.
2. Zhang, K.; Kleit, A.N. Mining rate optimization considering the stockpiling: A theoretical economics and real option model. *Resour. Policy* **2016**, *47*, 87–94. [[CrossRef](#)]
3. Samouhos, M.; Taxiarchou, M.; Pilatos, G.; Tsakiridis, P.E.; Devlin, E.; Pissas, M. Controlled reduction of red mud by H₂ followed by magnetic separation. *Miner. Eng.* **2017**, *105*, 36–43. [[CrossRef](#)]
4. Chun, T.; Long, H.; Li, J. Alumina-Iron Separation of High Alumina Iron Ore by Carbothermic Reduction and Magnetic Separation. *Sep. Sci. Technol.* **2015**, *50*, 760–766. [[CrossRef](#)]
5. Lu, L.; Holmes, R.J.; Manuel, J.R. Effects of alumina on sintering performance of hematite iron ores. *ISIJ Int.* **2007**, *47*, 349–358. [[CrossRef](#)]
6. Raghukumar, C.; Tripathy, S.K.; Mohanan, S. Beneficiation of Indian High Alumina Iron Ore Fines—A Case Study. *Int. J. Min. Eng. Miner. Proc.* **2012**, *1*, 94–100. [[CrossRef](#)]
7. Liu, Z.; Li, H. Metallurgical process for valuable elements recovery from red mud—A review. *Hydrometallurgy* **2015**, *155*, 29–43. [[CrossRef](#)]
8. Thella, J.S.; Mukherjee, A.K.; Srikakulapu, N.G. Processing of high alumina iron ore slimes using classification and flotation. *Powder Technol.* **2012**, *217*, 418–426. [[CrossRef](#)]
9. Chun, T.; Li, D.; Di, Z.; Long, H.; Tang, L.; Li, F.; Li, Y. Recovery of iron from red mud by high-temperature reduction of carbon-bearing briquettes. *J. S. Afr. Inst. Min. Metall.* **2017**, *117*, 361–364. [[CrossRef](#)]
10. Li, G.; Jiang, T.; Liu, M.; Zhou, T.; Fan, X.; Qiu, G. Beneficiation of High-Aluminium-Content Hematite Ore by Soda Ash Roasting. *Min. Proc. Extr. Met. Rev.* **2010**, *31*, 150–164. [[CrossRef](#)]
11. Chun, T.J.; Zhu, D.Q.; Pan, J.; He, Z. Preparation of metallic iron powder from red mud by sodium salt roasting and magnetic separation. *Can. Metall. Quart.* **2014**, *53*, 183–189. [[CrossRef](#)]
12. Sutar, H.; Mishra, S.C.; Sahoo, S.K.; Chakraverty, A.P.; Maharana, H.S. Progress of red mud utilization: An overview. *Am. Chem. Sci. J.* **2014**, *4*, 255–279. [[CrossRef](#)]
13. Wang, H.; She, X.; Zhao, Q.; Xue, Q.; Wang, J. Production of iron nuggets using iron-rich red mud by direct reduction. *Chin. J. Proc. Eng.* **2012**, *12*, 816–821.
14. Borra, C.R.; Blanpain, B.; Pontikes, Y.; Binnemans, K.; Van Gerven, T. Smelting of Bauxite Residue (Red Mud) in View of Iron and Selective Rare Earths Recovery. *J. Sustain. Met.* **2016**, *2*, 28–37. [[CrossRef](#)]
15. He, P.; Ju, D.; Shen, P.; Jin, H. Experimental research on comprehensive utilization of red mud based on direct reduction and melting by RHF iron bead technology. *Energ. Metall. Ind.* **2017**, *36*, 57–60.
16. Stjernberg, J.; Olivares-Oguz, M.A.; Antti, M.L.; Ion, J.C.; Lindblom, B. Laboratory scale study of the degradation of mullite/corundum refractories by reaction with alkali-doped deposit materials. *Ceram. Int.* **2013**, *39*, 791–800. [[CrossRef](#)]
17. Gan, L.; Xu, J.; Zhang, Z.; Liang, Y.; Wei, M.; Wen, C. Red Mud Pellets and Its Preparation Method. CN103602805A, 26 February 2014.
18. Shankar, A. Studies on High Alumina Blast Furnace Slags. Ph.D. Thesis, Royal Institute of Technology, Stockholm, Sweden, 15 June 2007.
19. Zhou, X.; Zhu, D.; Pan, J.; Luo, Y.; Liu, X. Upgrading of High-Aluminum Hematite-Limonite Ore by High Temperature Reduction-Wet Magnetic Separation Process. *Metals* **2016**, *6*, 57. [[CrossRef](#)]
20. Donskoi, E.; Olivares, R.I.; McElwain, D.L.S.; Wibberley, L.J. Experimental study of coal based direct reduction in iron ore/coal composite pellets in a one layer bed under nonisothermal, asymmetric heating. *Ironmak. Steelmak.* **2006**, *33*, 24–28. [[CrossRef](#)]
21. Zhu, D.; Luo, Y.; Pan, J.; Zhou, X. Reaction Mechanism of Siderite Lump in Coal-Based Direct Reduction. *High Temp. Mater. Process.* **2016**, *35*, 185–194. [[CrossRef](#)]

